Available online at www.sciencedirect.com
ScienceDirect
Journal of Solid State Chemistry 179 (2006) 3731–3738
JOURNAL OF SOLID STATE CHEMISTRY
www.elsevier.com/locate/jssc

Energetics of cobalt phosphate frameworks: α, β, and red $NaCoPO_4$

So-Nhu Le, Hank W. Eng, Alexandra Navrotsky*

Thermochemistry Facility and Chemistry Department, University of California, Davis, CA 95616, USA

Received 12 June 2006; received in revised form 1 August 2006; accepted 7 August 2006
Available online 12 August 2006

Abstract

Thermal behavior, relative stability, and enthalpy of formation of α (pink phase), β (blue phase), and red $NaCoPO_4$ are studied by differential scanning calorimetry, X-ray diffraction, and high-temperature oxide melt drop solution calorimetry. Red $NaCoPO_4$ with cobalt in trigonal bipyramidal coordination is metastable, irreversibly changing to α $NaCoPO_4$ at 827 K with an enthalpy of phase transition of $-17.4\pm6.9\,kJ\,mol^{-1}$. α $NaCoPO_4$ with cobalt in octahedral coordination is the most stable phase at room temperature. It undergoes a reversible phase transition to the β phase (cobalt in tetrahedra) at 1006 K with an enthalpy of phase transition of $17.6\pm1.3\,kJ\,mol^{-1}$. Enthalpy of formation from oxides of α, β, and red $NaCoPO_4$ are -349.7 ± 2.3, -332.1 ± 2.5, and $-332.3\pm7.2\,kJ\,mol^{-1}$; standard enthalpy of formation of α, β, and red $NaCoPO_4$ are -1547.5 ± 2.7, -1529.9 ± 2.8, and $-1530.0\pm7.3\,kJ\,mol^{-1}$, respectively. The more exothermic enthalpy of formation from oxides of β $NaCoPO_4$ compared to a structurally related aluminosilicate, $NaAlSiO_4$ nepheline, results from the stronger acid–base interaction of oxides in β $NaCoPO_4$ (Na_2O, CoO, P_2O_5) than in $NaAlSiO_4$ nepheline (Na_2O, Al_2O_3, SiO_2).

Keywords: $NaCoPO_4$; Cobalt phosphate framework; Enthalpy of formation; Phase transformation

1. Introduction

In the last decade, the discovery of a large variety of transition metal phosphates, especially with zeolitic or open framework structures, such as $(H_3NCH_2CH_2NH_3)_{0.5}CoPO_4$ with DAF and GIS frameworks [1,2], or $Zn_3(PO_4)_2(PO_3OH)(H_2DACH)$, a large pore structure with 24 member ring channels [3], has motivated further research in this class of materials. Similar to aluminosilicate zeolites, many transition metal phosphates with zeolitic or open framework structures can be synthesized by hydrothermal methods in the presence of organic templates [1–5]. Although their structures can be identified, factors that control structures, synthesis processes, and phase stabilities are still not well understood. Therefore, the synthesis of new structures mainly relies on trials of different organic templates and conditions.

Calorimetry is a powerful method to study energetic relationships among different structures. Previous studies of energetics of a large number of aluminosilicate zeolites, pure silica zeolites, and aluminophosphate zeolites provided knowledge to rationalize the stability and synthesis conditions of these materials [6–11]. However, trends in energetics of transition metal phosphates have not been investigated. Researchers believe that stabilities and synthesis conditions of transition metal phosphate frameworks should face some challenges that differ from aluminosilicate or aluminophosphate frameworks because transition metals have a greater tendency to form octahedral coordination [12]. Among zeolitic transition metal ions, cobalt (II) and zinc (II) are the most interesting because their electron configurations enable somewhat easier formation of tetrahedral coordination than for other transition metals. In order to study systematically the energetics of transition metal phosphate materials, we started with a study of the relationship between structures and stabilities of a simple inorganic transition metal phosphate, sodium cobalt (II) phosphate ($NaCoPO_4$).

Sodium cobalt (II) phosphate is known in four different structures. The first, α $NaCoPO_4$, determined by Hammond and Barbier [13], and the pink phase found by Feng

*Corresponding author. Fax: +530 752 9307.
E-mail address: anavrotsky@ucdavis.edu (A. Navrotsky).

0022-4596/$ - see front matter © 2006 Elsevier Inc. All rights reserved.
doi:10.1016/j.jssc.2006.08.007

et al. [14] have the same structure. α $NaCoPO_4$ crystallizes in the space group *Pnma*, consists of edge-sharing chains of CoO_6 octahedra cross-linked by PO_4 tetrahedra, and sodium ions are located in 10-coordinate cavities (Fig. 1a). The second polymorph is β $NaCoPO_4$ [13], also known as the blue phase [15]. Crystals of β $NaCoPO_4$ are twinned and belong to the space group $P6_1$ or $P6_5$. In this structure, CoO_4 and PO_4 tetrahedra alternately share corners to form a 3D framework with one-dimensional six ring channels, and sodium ions reside in these channels (Fig. 1b). Six member rings in β $NaCoPO_4$ are mixtures of UDUDUD and UUUDDD connections (U = up, D = down). The third polymorph crystallizes in the space group $P2_1/n$ and has the same tetrahedral connections as ABW zeolite [16]. In the red phase, the fourth polymorph, cobalt is in trigonal bipyramids connected with PO_4 tetrahedra to form a framework with one-dimensional channels (Fig. 1c) in the space group $P2_1/c$ [17]. However, reports on thermal properties of these polymorphs are inconsistent. Engel [18], Kolsi [19], and Toda et al. [20] indicate that the low-temperature phase (α) reversibly transforms to the high-temperature phase (β) at 998 K, and $NaCoPO_4$ melts at 1193 K. Feng et al. [14] reported that the red phase changes to the α phase at 983 K with an endothermic heat effect, and the α phase changes to β phase at 1193 K with an exothermic differential scanning calorimetry (DSC) peak.

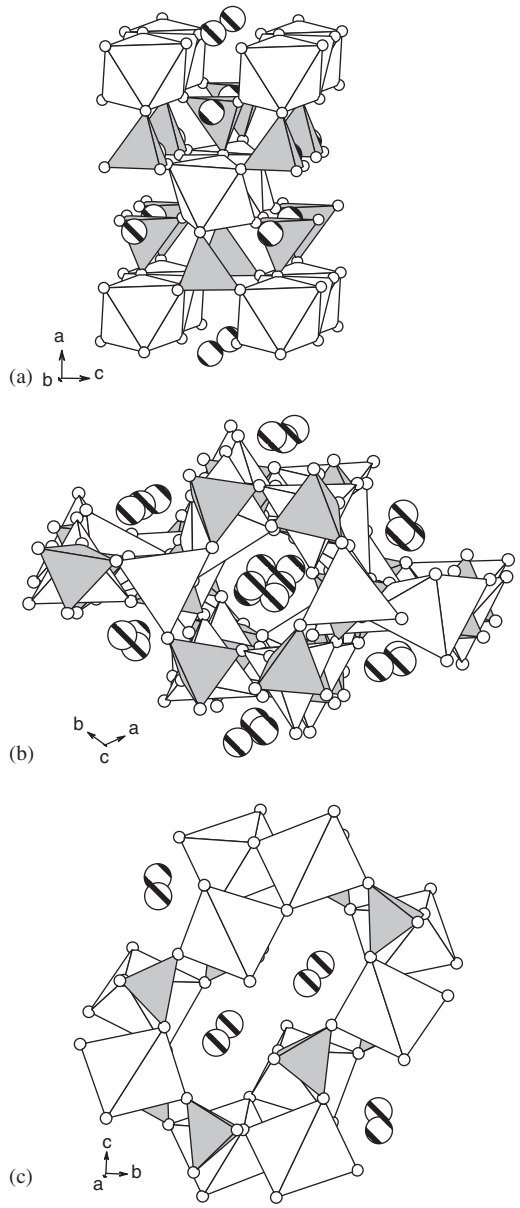

Fig. 1. Crystal structures of (a) α $NaCoPO_4$, (b) β $NaCoPO_4$, and (c) red $NaCoPO_4$. White polyhedra are cobalt oxide polyhedra, gray tetrahedra are PO_4, hatched circles are Na atoms, and white circles are O atoms.

By a combination of powder X-ray diffraction (XRD), DSC, and high-temperature oxide melt solution calorimetry, we clarify thermodynamic behavior of α, β, and red $NaCoPO_4$ in this paper. Their relative stabilities and enthalpies of formation are reported. Results address the question of how cobalt is stabilized in tetrahedral coordination compared to octahedral and trigonal bipyramidal coordination.

2. Experiments

2.1. Sample preparation

α and β $NaCoPO_4$ samples for calorimetric studies were synthesized by solid-state reaction. Powder $CoCO_3$ (Alfa Aesar, 99.5% metals basic) was mixed with a stoichiometric amount of solution of NaH_2PO_4 (Fisher, 98-102% $NaH_2PO_4 \cdot H_2O$). The mixture was stirred continuously and heated at 353–363 K to evaporate water. Carbon dioxide was also liberated during heating. The reactant mixture was dried at 373 K, ground, and heated at 623 K overnight to remove all volatilities. The powder obtained after heating at 623 K is blue in color. This blue powder was ground again, then pelletized and heated in platinum crucibles open to the air in a muffle furnace at suitable temperature until XRD patterns of quenched products matched the simulated powder patterns in the ICSD database [21]. α $NaCoPO_4$ was obtained as a gray powder after heating reactant pellets at 923 K for 3 days. β $NaCoPO_4$ was achieved after heating pellets of the α $NaCoPO_4$ at 1053 K for 3 days with an intermediate grinding. The color of the final ground β product is vivid violet blue.

We also attempted to isolate the red phase of $NaCoPO_4$ by following the hydrothermal method of Feng et al. [14,17]. In this method, the authors reported that in a container, crystals of the red and the pink phase grew into "star like clusters" that were easily separated. However, products of our hydrothermal trials after 4 days were mixtures of intergrown bulky crystals of α and red phase that could not be separated. These mixtures are black crystals that change to dark purple powder after grinding. When varying pH of reactant mixtures between 8 and 12 by

adjusting the amount of NaOH, with or without adding dimethylamine, and lengthening the reaction time up to 8 days, we always obtained the pure α phase. These as-synthesized α products are also in the form of black crystals that become gray powder upon grinding. One sample of the mixture of red and α phase, and another sample of pure α phase synthesized by the hydrothermal method were also involved in the characterization and calorimetric measurements in this study. All samples were kept in sealed vials placed in a desiccator containing $CaCl_2$ to avoid adsorption of water from the air.

2.2. Sample characterization

XRD patterns of powder samples were collected on a Scintag PAD-V diffractometer using Cu*K*α radiation, and operating at 45 kV and 40 mA. Data were collected in the step scan mode with 2θ ranging from 10° to 60°, a step size of 0.02°, and a dwell time of 5 s step^{-1}. Quartz was used as an external standard for calibration of the diffractometer. Powder simulation patterns from the ICSD database [21] were used as references for phase identification. Lattice parameters of single-phase samples were calculated from XRD patterns using JADE software [22]. For the sample, which is mixture of red and α phases, the Rietveld method [23,24] was used to refine the XRD data. Full Rietveld refinements were completed by using the EXP-GUI/GSAS software package [25,26]. Initial structural models of the red phase and the α phase were taken from single-crystal data of Feng et al. [14,17]. The lattice parameters, atomic displacements, peak profile parameters, and scale factor were allowed to freely vary in all refinements. Because there are some overlapping peaks of the α and the red phase, soft constraints were applied for the refinement of atomic positions of both phases. The atomic displacements of each atom type in each phase were constrained to be equal.

Chemical composition of samples was determined using a Cameca SX-100 electron microprobe. Because α and β samples produced by solid-state method were made from the same batch of reactant, only the β sample was analyzed. Powder of the β sample was pelletized and annealed at 1073 K overnight before being polished. Samples produced from hydrothermal methods were in the form of micron-sized crystals; therefore, they were polished without pelletizing or annealing. A wide beam was applied for microprobe analysis to avoid evaporation or migration of sodium in samples. Between 8 and 12 points were analyzed for each sample. Jadeite, cobalt metal, and apatite were used as standards for sodium, cobalt, and phosphate, respectively.

The content of Co^{3+} was determined by iodometric titration. About 80 mg of each sample was dissolved in acidic KI solution, and titrated by standardized thiosulfate solution. Recrystallized KIO_3 (Alfa Aesar, 99.4–100.4%) dried at 450 K was used as the primary standard in this titration.

2.3. DSC and thermogravimetric analysis

To clarify the discrepancy in thermal behavior of polymorphs of $NaCoPO_4$ in previous papers [13,14,18–20], and to determine water content in samples, DSC and TGA of samples were performed on a Netzsch STA 449 instrument. Pellets weighing about 50 mg were heated in a platinum crucible from 303 to 1273 K in argon atmosphere with a heating rate of 10 K min^{-1}, and an argon flow rate of 40 cm^3 min^{-1}. A calculation of the enthalpy of phase transitions from DSC was not attempted because of the incompleteness of phase transitions under thermal analysis conditions (see below).

2.4. High-temperature oxide melt calorimetry

To determine relative stability and heat of formation of different polymorphs of $NaCoPO_4$, drop solution calorimetry using a molten oxide as solvent was performed in a custom built Tian–Calvet twin calorimeter. The instrument, experiments, and thermochemical applications have been described previously [27,28].

In a drop solution experiment, an accurately weighed pellet of about 5 mg was dropped from room temperature into 20 g of molten sodium molybdate ($3Na_2O \cdot 4MoO_3$) solvent in the calorimeter at 973 K. Argon gas was bubbled through the solvent continuously at a rate of 5 cm^3 min^{-1} to facilitate the dissolution and to avoid the local saturation of solute in the melt. Another flow of argon at 30 cm^3 min^{-1}was flushed steadily above the solvent to sweep the gas out of the calorimeter. Under these conditions, all dissolved cobalt is divalent [28,29]. The heat of drop solution (ΔH_{ds}) measured in this experiment is the sum of: (1) the enthalpy of heating the sample from room temperature to calorimeter temperature (heat content), (2) the enthalpy of any phase transition that occurs on heating, and (3) the enthalpy of dissolving the sample into the solvent at the calorimeter temperature. At least eight measurements were performed for each sample. Calibration for enthalpy measurement in the calorimeter is based on the heat content of corundum. This was accomplished by dropping 5 mg pellets of corundum (Aldrich, 99.99% Al_2O_3; heated overnight at 1773 K) from room temperature into empty platinum crucibles in the calorimeter as described in earlier works [28].

3. Results and discussion

3.1. Characterization of samples

Chemical compositions of samples from microprobe analysis presented in Table 1 show they have the ideal stoichiometry of $NaCoPO_4$ within experimental errors. All samples have less than 0.09% of cobalt presented as Co^{3+}. The TGA performed on the same day as calorimetric measurement showed no weight loss in solid-state samples and less than 0.1% weight loss for hydrothermal products.

Table 1
Chemical composition of samples from microprobe analysis

Sample	Chemical composition (weight percent)		
	Na_2O	CoO	P_2O_5
α-$NaCoPO_4$ (hy)	17.7±0.3	42.0±0.4	40.1±0.2
β-$NaCoPO_4$ (ss)	17.6±0.4	42.0±0.3	39.9±0.4
Mixture-$NaCoPO_4$ (hy)	17.5±0.2	42.6±0.4	39.4±0.3
Theoretical	17.5	42.4	40.1

(ss): sample prepared by solid state method, (hy): sample prepared by hydrothermal method.
Uncertainties are two standard deviations of the means from 8 to 12 analyzed points.

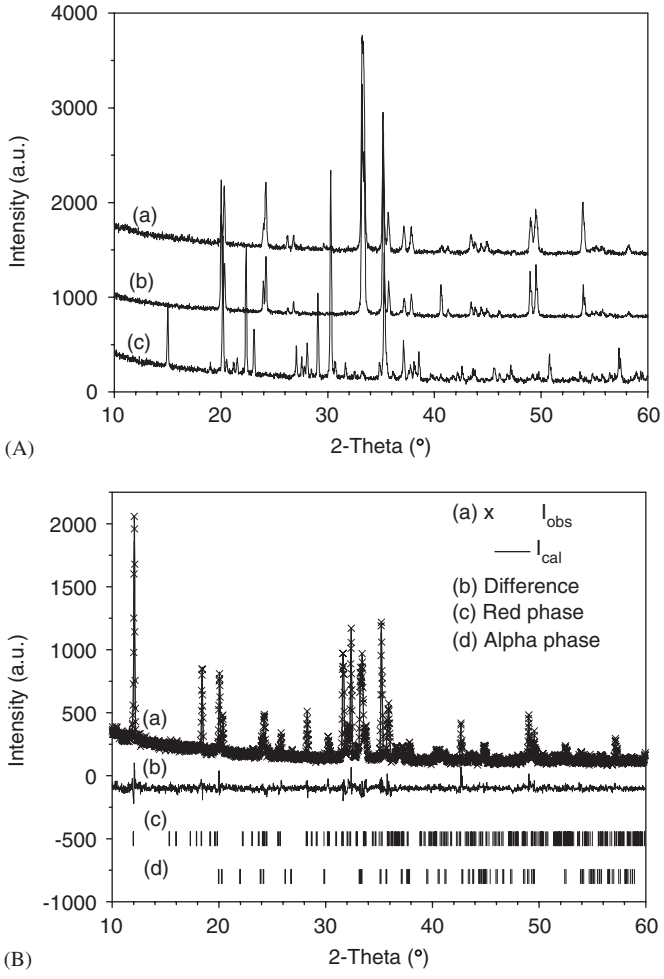

Fig. 2. (A) XRD patterns of single-phase samples: (a) α $NaCoPO_4$ from solid-state method, (b) α $NaCoPO_4$ from hydrothermal synthesis, and (c) β $NaCoPO_4$ from solid-state method. (B) Observed, calculated, difference patterns, and Bragg angle positions (as tick marks) of the Rietveld refinement of the mixture of red and α $NaCoPO_4$ sample.

Although the color of our α samples is black or gray black, that is somewhat different from previous reports of light pink [13,14,18–20], there is no evidence of an impurity phase in our samples, and the content of Co^{3+} and water is very low. Therefore, we assume compositions of all samples are $NaCoPO_4$.

Powder XRD patterns of α and β samples show that they are pure phases (Fig. 2A). Their calculated crystallographic data are summarized in Table 2. These data agree well with those found from single crystals [13–15]. Observed, calculated, and difference patterns of the Rietveld refinement of the mixture sample are presented in Fig. 2B. There are 2499 observations and 83 variables in this refinement. Residual functions and the "goodness of fit" value of the refinement are $R_p = 7.43\%$, $wR_p = 9.53\%$, and $\chi^2 = 2.02$. Weight fractions of the red and the α phase at the end of the refinement are 0.552 and 0.448, respectively, with the uncertainty of ±0.011 (estimated standard deviation from GSAS calculation [26]). Lattice parameters of each phase in this sample are presented in Table 2.

3.2. Thermal behavior of α, β, and red $NaCoPO_4$

Both α $NaCoPO_4$ samples produced from solid-state and from hydrothermal method display the same DSC behavior. The DSC curve of the α sample from solid-state synthesis (Fig. 3a) shows two endothermic peaks at 1006 and 1214 K (all phase transition temperatures reported in this paper associate with peak temperatures). The first endothermic peak associates with the phase transition from α to β, as confirmed by XRD. The second endothermic peak accompanies the melting of $NaCoPO_4$, which is easy to recognize after DSC experiments.

The β sample also shows two endothermic peaks in its DSC trace similar to the α sample and an additional exothermic peak at 752 K (Fig. 3b). The XRD pattern of a β sample after heating overnight at 823 K and quenching to room temperature showed a mixture of a main α phase and minor β phase. Therefore, this exothermic peak associates with the transformation from β to α. These data strongly support the reversible phase transition from α to β $NaCoPO_4$ near 998 K and melting temperature about 1193 K proposed by Engel [18], Kolsi [19], and Toda et al. [20]. These observations support the prediction that the α phase is thermodynamically stable with respect to the β phase at low temperature.

The mixture of red and α $NaCoPO_4$ displays a similar DSC trace to the β sample, but the exothermic peak shifts to 827 K (Fig. 3c). The XRD pattern of this sample after heating in a muffle furnace at 973 K and quenching to room temperature showed pure α $NaCoPO_4$. Therefore, the exothermic peak at 827 K is assigned to the irreversible phase transition from red to α $NaCoPO_4$. This α phase undergoes a thermodynamically reversible phase transition to the β phase when heated. There is evidence neither of a reversible transition between the α and red phase nor of a direct transition from red to β phase. It is clear that the red phase is metastable. Relative stabilities of α, β, and red $NaCoPO_4$ are confirmed by our drop solution results below.

Table 2
Crystallographic data calculated from JADE (for single phase samples) and GSAS (for the mixture sample)

Sample	Space group	Lattice parameters				ρ_{cal} (g cm^{-3})
		a (Å)	b (Å)	c (Å)	β (°)	
α-$NaCoPO_4$ (ss)	*Pnma*	8.878(1)	6.795(1)	5.0288(7)	90	3.873
α-$NaCoPO_4$ (hy)	*Pnma*	8.879(2)	6.793(1)	5.0289(7)	90	3.874
β-$NaCoPO_4$ (ss)	$P6_1$	10.167(1)	10.167(1)	23.872(3)	90	3.299
Mixture-$NaCoPO_4$ (hy)	$P2_1/c$	5.7801(8)	11.0867(5)	9.9187(7)	92.69(2)	3.701
	Pnma	8.8906(4)	6.7996(6)	5.0329(4)	90	3.863

(ss): sample prepared by solid state method, (hy): sample prepared by hydrothermal method.
Numbers in parentheses are estimated standard deviations from JADE or GSAS calculation.

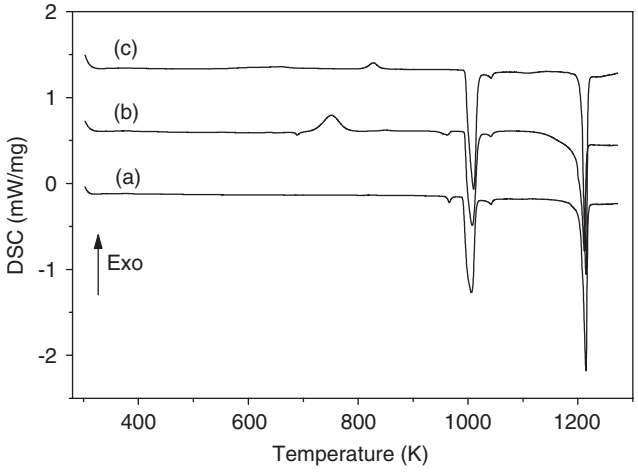

Fig. 3. DSC traces of (a) α $NaCoPO_4$, (b) β $NaCoPO_4$, and (c) mixture of red and α $NaCoPO_4$.

3.3. Enthalpies of drop solution of α, β, and red $NaCoPO_4$ in molten sodium molybdate at 973 K

Under bubbling gas, the dissolution of $NaCoPO_4$ in sodium molybdate at 973 K occurred smoothly in about 30 min and produced repeatable results. Enthalpies of drop solution of two α samples, one prepared from solid-state and the other from hydrothermal method, are 174.65 ± 0.86 and 173.32 ± 0.97 kJ mol^{-1}, respectively (in this paper, uncertainties of all enthalpy measurements are reported as twice of the standard deviation of the mean). Applying t-test at 95% confidence level to compare these two experimental means, there is no significant difference between them. Therefore, the average value of enthalpy of drop solution of α phase, 173.99 ± 0.65 kJ mol^{-1}, is used for further discussion. Note that we use propagation of errors following Miller and Miller [30] to estimate uncertainties of computed values in this paper.

The β and the mixture of α and red phases produce significantly less endothermic enthalpies of drop solution than α samples. Their enthalpies of drop solution are 156.39 ± 1.07 and 164.37 ± 1.09 kJ mol^{-1} for the β and the mixture sample respectively. Because we could not isolate the red phase of $NaCoPO_4$, the enthalpy of solution of the red phase is calculated from values of enthalpies of drop solution of the pure α phase and the mixture of red and α phases by the following equation, where x and y are weight fractions of the red phase and the α phase, respectively, from Rietveld refinement:

$$\Delta H_{ds}(\text{red} - NaCoPO_4) = 1/x\Delta H_{ds}\,(\text{mixture} - NaCoPO_4) - y/x\Delta H_{ds}\,(\alpha - NaCoPO_4). \quad (1)$$

Consequently, the heat of drop solution of the red phase is determined to be 156.56 ± 6.86 kJ mol^{-1}. The large uncertainty results mainly from standard deviations of weight fractions. As we will see later, energetic data related to red $NaCoPO_4$ always have larger uncertainties than α and β phases because of that contribution.

3.4. Energetics of phase transitions and relative stability of α, β, and red $NaCoPO_4$

Enthalpies of phase transformation from red to α $NaCoPO_4$, and from α to β $NaCoPO_4$ at room temperature, are represented by following reactions:

$$\text{red-}NaCoPO_4(\text{cr}, 298\,\text{K}) \rightarrow \alpha\text{-}NaCoPO_4(\text{cr}, 298\,\text{K})\quad \Delta H_{tr}(\text{red} \rightarrow \alpha), 298\,\text{K} \quad (2)$$

$$\alpha\text{-}NaCoPO_4(\text{cr}, 298\,\text{K}) \rightarrow \beta\text{-}NaCoPO_4(\text{cr}, 298\,\text{K})\quad \Delta H_{tr}(\alpha \rightarrow \beta), 298\,\text{K} \quad (3)$$

Applying cycles A and B in Table 3, enthalpies of transition from red to α phase, and from α to β phase are determined to be $\Delta H_{tr(\text{red}\rightarrow\alpha),\ 298\,K} = -17.4 \pm 6.9$ kJ mol^{-1} and $\Delta H_{tr(\alpha\rightarrow\beta),298\,K} = 17.6 \pm 1.3$ kJ mol^{-1}. These results confirm the exothermic peak of red—α transition at 827 K and the endothermic peak presented for α–β transition at 1006 K on DSC traces. It is clear that cobalt in $NaCoPO_4$ is stabilized in octahedral coordination compared to tetrahedral or trigonal bipyramidal coordination. Furthermore, energetic differences of cobalt in $NaCoPO_4$ in different geometries are relatively small, especially the difference between cobalt in tetrahedral

Table 3
Thermodynamic cycles used for energetic calculations

Cycle A: Thermodynamic cycle for the enthalpy of phase transition from red to α $NaCoPO_4$ at room temperature	
Red-$NaCoPO_4$ (cr, 298 K) → $NaCoPO_4$ (sol, 973 K)	ΔH_{ds}(red-$NaCoPO_4$)
α-$NaCoPO_4$ (cr, 298 K) → $NaCoPO_4$ (sol, 973 K)	ΔH_{ds}(α-$NaCoPO_4$)
Red-$NaCoPO_4$ (cr, 298 K) → α-$NaCoPO_4$ (cr, 298 K)	$\Delta H_{tr(red\rightarrow\alpha),\ 298\,K}$
$\Delta H_{tr(red\rightarrow\alpha),\ 298\,K} = \Delta H_{ds}$(red-$NaCoPO_4$) − ΔH_{ds}(α-$NaCoPO_4$)	
Cycle B: Thermodynamic cycle for the enthalpy of phase transition from α to β $NaCoPO_4$ at room temperature	
α-$NaCoPO_4$ (cr, 298 K) → $NaCoPO_4$ (sol, 973 K)	ΔH_{ds}(α-$NaCoPO_4$)
β-$NaCoPO_4$ (cr, 298 K) → $NaCoPO_4$ (sol, 973 K)	ΔH_{ds}(β-$NaCoPO_4$)
α-$NaCoPO_4$ (cr, 298 K) → β-$NaCoPO_4$ (cr, 298 K)	$\Delta H_{tr(\alpha\rightarrow\beta),\ 298\,K}$
$\Delta H_{tr(\alpha\rightarrow\beta),\ 298\,K} = \Delta H_{ds}$(α-$NaCoPO_4$) − ΔH_{ds}(β-$NaCoPO_4$)	
Cycle C: Thermodynamic cycle for the enthalpy of formation from oxides of $NaCoPO_4$.	
$NaCoPO_4$ (cr, 298 K) → $NaCoPO_4$ (sol, 973 K)	ΔH_{ds} ($NaCoPO_4$)
Na_2O (cr, 298 K) → Na_2O (sol, 973 K)	ΔH_{ds} (Na_2O)
CoO (cr, 298 K) → CoO (sol, 973 K)	ΔH_{ds} (CoO)
P_2O_5 (cr, 298 K) → P_2O_5 (sol, 973 K)	ΔH_{ds} (P_2O_5)
$\frac{1}{2}Na_2O$ (cr, 298 K) + CoO (cr, 298 K) + $\frac{1}{2}P_2O_5$ (cr, 298 K) → $NaCoPO_4$ (cr, 298 K)	$\Delta H_{f-ox,\ 298\ K}$ ($NaCoPO_4$)
$\Delta H_{f-ox,\ 298\,K}$ ($NaCoPO_4$) = $\frac{1}{2}\Delta H_{ds}$ (Na_2O) + ΔH_{ds} (CoO) + $\frac{1}{2}\Delta H_{ds}$ (P_2O_5) − ΔH_{ds} ($NaCoPO_4$)	

coordination in the β phase and trigonal bipyramidal coordination in the red phase ($0.2 \pm 6.9\,kJ\,mol^{-1}$). These enthalpy differences among $NaCoPO_4$ polymorphs are similar to enthalpy differences between zeolites and dense phases of the same composition [6–9]. This explains observations of Feng et al. [14,15,17] that α and red, as well as β and red, may coexist in hydrothermal synthesis products. They also explain our observation that when lengthening reaction time, hydrothermal synthesis products become pure α phase instead of mixtures of red and α.

Cobalt is also in octahedral coordination in rock-salt CoO and tetrahedral coordination in zinc blende and wurtzite CoO [31]. Grimes and Lagerlof [32] calculated lattice energies of CoO in different structures and found that rock-salt CoO was 38 and $26\,kJ\,mol^{-1}$ more stable than zinc-blende and wurtzite, respectively. Later, by oxide melt drop solution calorimetry, rock-salt CoO was experimentally determined to be $37 \pm 5\,kJ\,mol^{-1}$ more stable in enthalpy than zinc-blende CoO [31]. Thus, the energetic difference between octahedral CoO_6 and tetrahedral CoO_4 in CoO is about twice as large as the difference in $NaCoPO_4$. In other words, sodium and phosphate ions promote the stabilization of cobalt in a tetrahedral oxo environment compared to the octahedral environment that is more stable in the binary oxide. This result is promising for the synthesis of other cobalt phosphate compounds with cobalt in tetrahedral coordination, especially when sodium is replaced by larger alkali ions [15,33,34].

The entropy of the reversible phase transition between α and β phases is calculated to be $17.5 \pm 1.3\,J\,mol^{-1}\,K^{-1}$ since $\Delta G_{tr} = 0$ at the temperature of phase transition (here, the temperature on the DSC trace of the α phase, 1006 K). The positive value of entropy of phase transition reflects the increase in molar volume or decrease in density of two phases involved in the phase transition. Considering symmetries, densities, and relative stabilities of α and β $NaCoPO_4$, our results are in agreement with the general expectation of a reversible phase transition in which the less dense phase (here, β $NaCoPO_4$) possesses the higher symmetry and is stabilized at higher temperature. However, this behavior is not exhibited for the irreversible phase transition of red and α $NaCoPO_4$. In this case, the metastable phase (the red phase) also possesses a less dense structure, but a lower symmetry space group than the stable phase (α phase).

3.5. Enthalpy of formation of $NaCoPO_4$

Enthalpy of formation of different polymorphs of $NaCoPO_4$ from their oxides ($\Delta H_{f-ox,\ 298\,K}$) is reported by reaction (4):

$$\tfrac{1}{2}Na_2O(cr, 298\,K) + CoO(cr, 298\,K) + \tfrac{1}{2}P_2O_5(cr, 298\,K) \rightarrow NaCoPO_4(cr, 298\,K). \quad (4)$$

Standard enthalpy of formation of $NaCoPO_4$ ($\Delta H^{o}_{f298\,K}$ ($NaCoPO_4$), enthalpy of formation from elements) can be derived from $\Delta H_{f-ox,\ 298\,K}$ ($NaCoPO_4$) and standard enthalpy of formation of relevant oxides by Eq. (5):

$$\Delta H^{o}_{f}, 298\,K(NaCoPO_4) = \Delta H_{f\text{-}ox,298\,K}(NaCoPO_4) + \tfrac{1}{2}\Delta H^{o}_{f,298\,K}(Na_2O) + \Delta H^{o}_{f,298\,K}(CoO) + \tfrac{1}{2}\Delta H^{o}_{f,298\,K}(P_2O_5). \quad (5)$$

Using Eq. (5), thermodynamic cycle C in Table 3, and auxiliary values of enthalpy of drop solution and standard enthalpy of formation of oxides, values of enthalpy of formation from oxides ($\Delta H_{f-ox,\ 298\ K}$) and from elements ($\Delta H^{o}_{f,\ 298\,K}$) of α, β, and red $NaCoPO_4$ are calculated. All thermodynamic data are summarized in Table 4.

Research in cobalt phosphates is motivated in part because their framework structures are similar to those of

Table 4
Summary of thermodynamic data used in this paper

Compound	ΔH_{ds} (kJ mol^{-1})	$\Delta H_{f-ox,\ 298\ K}$ (kJ mol^{-1})	$\Delta H^{o}_{f,\ 298\ K}$ (kJ mol^{-1})
Na_2O (cr)	−217.56±4.25 [35]	N/A	−414.8±0.3 [37]
CoO (cr)	15.35±0.46 [29]	N/A	−237.9±1.3 [37]
P_2O_5 (cr)	−164.60±0.85 [36]	N/A	−1504.9±0.5 [37]
α-$NaCoPO_4$ (cr)	173.99±0.65	−349.7±2.3	−1547.5±2.7
β-$NaCoPO_4$ (cr)	156.39±1.07	–332.1±2.5	−1529.9±2.8
Red-$NaCoPO_4$ (cr)	156.56±6.86	−332.3±7.2	−1530.0±7.3

ΔH_{ds}, enthalpy of drop solution in sodium molybdate at 973 K; $\Delta H_{f-ox,\ 298\ K}$, enthalpy of formation from oxides; and $\Delta H^{o}_{f,\ 298\,K}$, standard enthalpy of formation (enthalpy of formation from elements).Values without cited reference are from this work.

aluminosilicate zeolites. Therefore, it is interesting to compare the energetics of aluminosilicate and cobalt phosphate. Nepheline $NaAlSiO_4$ and β $NaCoPO_4$ are chosen because both of them have structures built from alternating connections of tetrahedral AlO_4 and SiO_4, and CoO_4 and PO_4, respectively. The only difference in tetrahedral connections of two structures is that six member rings of $NaAlSiO_4$ are UDUDUD connections instead of a mixture of UDUDUD and UUUDDD connections in β $NaCoPO_4$. Enthalpy of formation from oxides of $NaAlSiO_4$ nepheline is −134.4 kJ mol^{-1} [9], less exothermic than of β $NaCoPO_4$, −332.1 kJ mol^{-1} (this work, Table 4). This indicates that interactions of oxides in β $NaCoPO_4$ is stronger than in nepheline. Considering differences in oxidation states between Al (+3) and Si (+4) in nepheline, and between Co (+2) and P (+5) in β $NaCoPO_4$, it is clear that acid–base interactions in β $NaCoPO_4$ are stronger than in nepheline. This may be an important factor in stabilizing divalent cobalt in a tetrahedral environment.

4. Conclusion

Thermal behavior, enthalpy of phase transition, and enthalpy of formation from oxides and from elements of three different polymorphs of $NaCoPO_4$ have been determined. While red $NaCoPO_4$ is a metastable phase with cobalt in trigonal bipyramid coordination, α $NaCoPO_4$ with cobalt in octahedral coordination is the stable phase at low temperature, and β $NaCoPO_4$ with cobalt in tetrahedral coordination is the stable phase at high temperature. Although cobalt is most enthalpically stable in octahedral coordination, differences in enthalpies of cobalt in octahedral, tetrahedral, and trigonal bipyramidal are relatively small in the presence of sodium and phosphorous oxides. Acid–base interactions of oxides in $NaCoPO_4$ may be an important factor in stabilizing cobalt in tetrahedral environment.

Acknowledgments

This work was supported by National Science Foundation under Grants DMR 01-01391 and DMR 06-01892. We thank Dr. Sarah Roeske for microprobe analysis, Dr. Lena Mazeina and Dr. Yosuke Moriya for translating German and Japanese papers.

Reference

[1] J. Chen, R.H. Jones, S. Natarajan, M.B. Hursthouse, J.M. Thomas, Angew. Chem. Int. Ed. Engl. 33 (1994) 639–640.
[2] H.-M. Yuan, J.-S. Chen, G.-S. Zhu, J.-Y. Li, J.-H. Yu, G.-D. Yang, R.-R. Xu, Inorg. Chem. 39 (2000) 1476–1479.
[3] G.-Y. Yang, S.C. Sevov, J. Am. Chem. Soc. 121 (1999) 8389–8390.
[4] R. Szostak, Molecular Sieves: Principles of Synthesis and Identification, 2nd ed, Blackie Academic & Professional, New York, 1998.
[5] A.K. Cheetham, G. Ferey, T. Loiseau, Angew. Chem. Inter. Ed. Engl. 38 (1999) 3268–3292.
[6] P.M. Piccione, C. Laberty, S. Yang, M.A. Camblor, A. Navrotsky, M.E. Davis, J. Phys. Chem. B 104 (2000) 10001–10011.
[7] P.M. Piccione, B.F. Woodfield, J. Boerio-Goates, A. Navrotsky, M.E. Davis, J. Phys. Chem. B 105 (2001) 6025–6030.
[8] P.M. Piccione, S. Yang, A. Navrotsky, M.E. Davis, J. Phys. Chem. B 106 (2002) 3629–3638.
[9] A. Navrotsky, Z.-R. Tian, Chemistry, Weinheim an der Bergstrasse, Germany, vol. 7, 2001, pp. 769–774.
[10] Y. Hu, A. Navrotsky, C.-Y. Chen, M.E. Davis, Chem. Mater. 7 (1995) 1816–1823.
[11] A. Navrotsky, J. Therm. Anal. Calorim. 57 (1999) 653–658.
[12] F.A. Cotton, G. Wilkinson, Advance Inorganic Chemistry, 5th ed, Wiley, New York, 1988.
[13] R. Hammond, J. Barbier, Acta Crystallogr. B 52 (1996) 440–449.
[14] P. Feng, X. Bu, G. Stucky, J. Solid State Chem. 131 (1997) 160–166.
[15] P. Feng, X. Bu, S.H. Tolbert, G. Stucky, J. Am. Chem. Soc. 119 (1997) 2497–2504.
[16] A.M. Chippindale, A.R. Cowley, J. Chen, Q. Gao, R. Xu, Acta Crystallogr. C 55 (1999) 845–847.
[17] P. Feng, X. Bu, G.D. Stucky, J. Solid State Chem. 129 (1997) 328–333.
[18] G. Engel, Neues Jahbr. Mineral. Abh. 127 (1976) 197–211.
[19] A.-W. Kolsi, C.R. Acad, Sc. Ser. IIC: Chim. 286 (1978) 249–251.
[20] Y. Toda, K. Hashimoto, K. Hashimoto, Y. Arai, Gypsum Lime 206 (1987) 10–22.
[21] Inorganic Crystal Structure Database, National Institute of Standards and Technology, Version 1.3.3, 2004.
[22] MDI Materials Database, JADE 6.
[23] H.M. Rietveld, Acta Crystallogr. 22 (1967) 151.
[24] H.M. Rietveld, J. Appl. Cryst. 2 (1969) 65.
[25] B.H. Toby, J. Appl. Cryst. 34 (2001) 210.
[26] A.C. Larson, R.B. Von Dreele, General structure analysis system, Los Alamos National Laboratory Report LAUR 86-748, 2004.

[27] A. Navrotsky, in: C.M. Gramaccioli (Ed.), Energy Modelling in Minerals: University Textbook, Eotvos University Press, Budapest, 2002, pp. 5–31.
[28] A. Navrotsky, Phys. Chem. Minerals 24 (1997) 222–241.
[29] M. Wang, A. Navrotsky, Solid State Ionics 166 (2004) 167–173.
[30] J.N. Miller, J.C. Miller, Statistics and Chemometrics for Analytical Chemistry, 4th ed, Prentice-Hall, New York, 2000.
[31] J. DiCarlo, A. Navrotsky, J. Am. Ceram. Soc. 76 (1995) 2465–2467.
[32] R.W. Grimes, K.P.D. Lagerlof, J. Am. Ceram. Soc. 74 (1991) 270–273.
[33] B. Elouadi, L. Elammari, Ferroelectrics 107 (1990) 253–258.
[34] P.F. Henry, E.M. Hughes, M.T. Weller, Dalton 4 (2000) 555–558.
[35] F. Tessier, A. Navrotsky, A. Sauze, R. Marchand, Chem. Mater. 12 (2000) 148–154.
[36] S.V. Ushakov, K.B. Helean, A. Navrotsky, L.A. Boatner, J. Mater. Res. 16 (2001) 2623–2633.
[37] R.A. Robie, B.S. Hemingway, Thermodynamic Properties of Minerals and Related Substances at 298.15 K and 1 Bar (10^5 Pascals) Pressure and at Higher Temperatures, United States Government Printing Office, Washington, 1995.